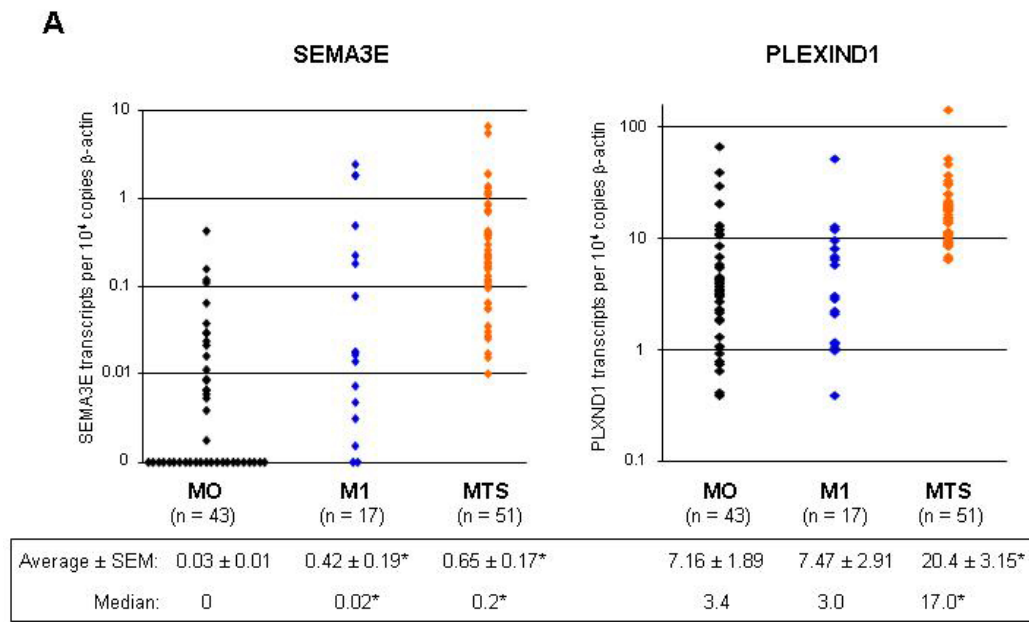


**Sema3E-PlexinD1 signaling drives cancer cell invasiveness
and metastatic spreading in vivo**

Casazza et al.

SUPPLEMENTAL FIGURES

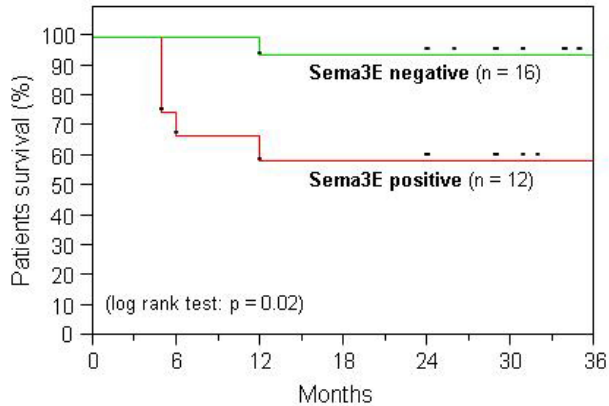
Figure S1



B

sample	Sema3E			PlexinD1		
	primary tum.	metastasis		primary tum.	metastasis	
#1	0,1804	0,0183	decrease	0,6411	8,2920	increase
#3	0,0018	0,0033	increase	0,2842	0,9522	increase
#4	0,0017	0,0235	increase	0,2224	2,0707	increase
#33	0,0014	0,0026	increase	0,1132	0,2297	increase
#34	0,1834	0,0553	decrease	0,5667	2,5658	increase
#52	0,0001	0,0015	increase	0,0975	0,2947	increase
#53	0,0005	0,1160	increase	0,0387	0,7702	increase
#54	0,0007	0,0147	increase	0,9584	4,1243	increase
Median	0.002	0.017	increase	0.105	0.532	increase

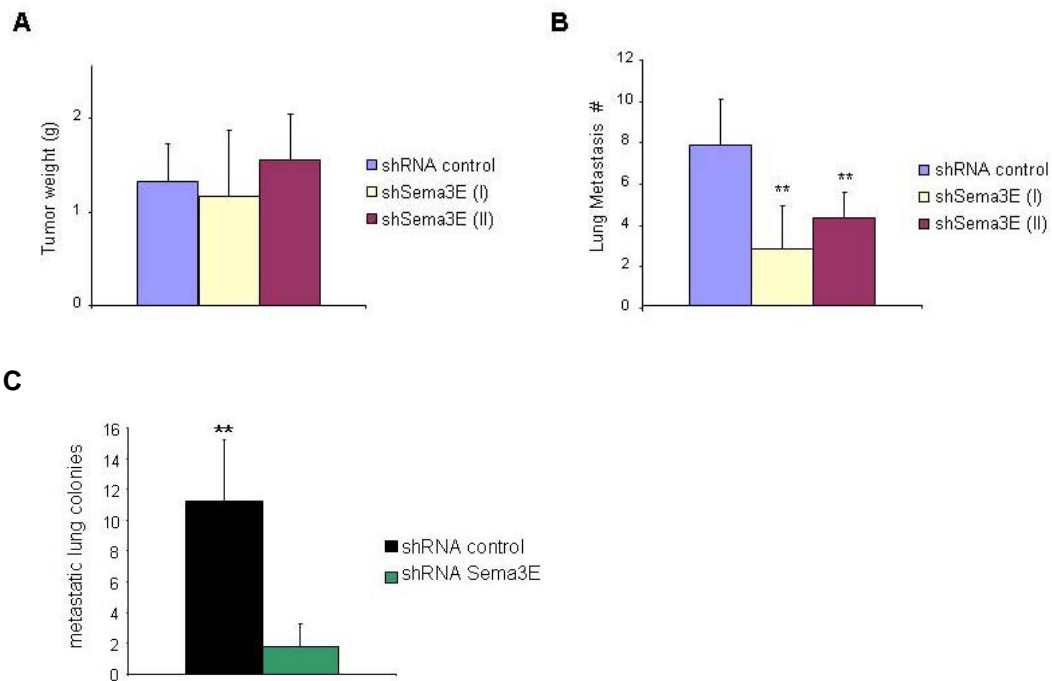
C



A-C. Sema3E and PlexinD1 mRNA expression was analyzed by TaqMan quantitative RT-PCR in tissue samples derived from resected primary colorectal adenocarcinoma, or liver metastases from colorectal carcinoma. The panel included: 43 primary tumors that had not formed distant metastases (*M0* stage according to TNM classification for colorectal cancer), 17 primary colorectal tumors that had formed distant metastases at the time of resection (*M1* stage), and 51 liver metastases (*MTS*). Cancer differentiation grades (well, moderately and poorly differentiated), and stages of local invasiveness or lymph node metastases (according to according to TNM classification for colorectal cancer) were equally distributed among primary *M0* and *M1* tumor samples (not shown). Panel **A**) shows the distribution of individual samples (either *M0*, *M1* or *MTS*) based on the estimated number of gene transcripts (relative to 10^4 copies of β -actin, used as internal reference). Y-axis uses a logarithmic scale. Note that Sema3E expression is below detection threshold in a large fraction of non-metastatic *M0* tumors. Panel **B**) shows Sema3E and PlexinD1 expression in a limited panel of matched samples of primary colorectal carcinomas and liver metastasis derived from the same patient. The table shows the estimated number of gene transcripts per 10^3 copies of β -actin. Sema3E and PlexinD1 expression was increased in 75% and 100% metastasis, respectively, compared to corresponding primary tumors. Statistical significance could be confirmed by Wilcoxon test for PlexinD1 ($p= 0.004$).

Panel C) shows available data on the overall survival of a subset of 28 colon carcinoma patients, clustered on the bases of *Sema3E* expression in the excised primary tumor samples. Kaplan-Meier curves indicate significantly increased mortality rates of patients with *Sema3E*-positive colorectal tumors (red line) compared to patients with *Sema3E*-negative tumors (green line)($p = 0.02$ according to the log rank test; $n = 12/16$). Dots on the lines indicate death of a patient, dots above the lines represent censored patients. The median follow-up for all surviving patients was 31 months.

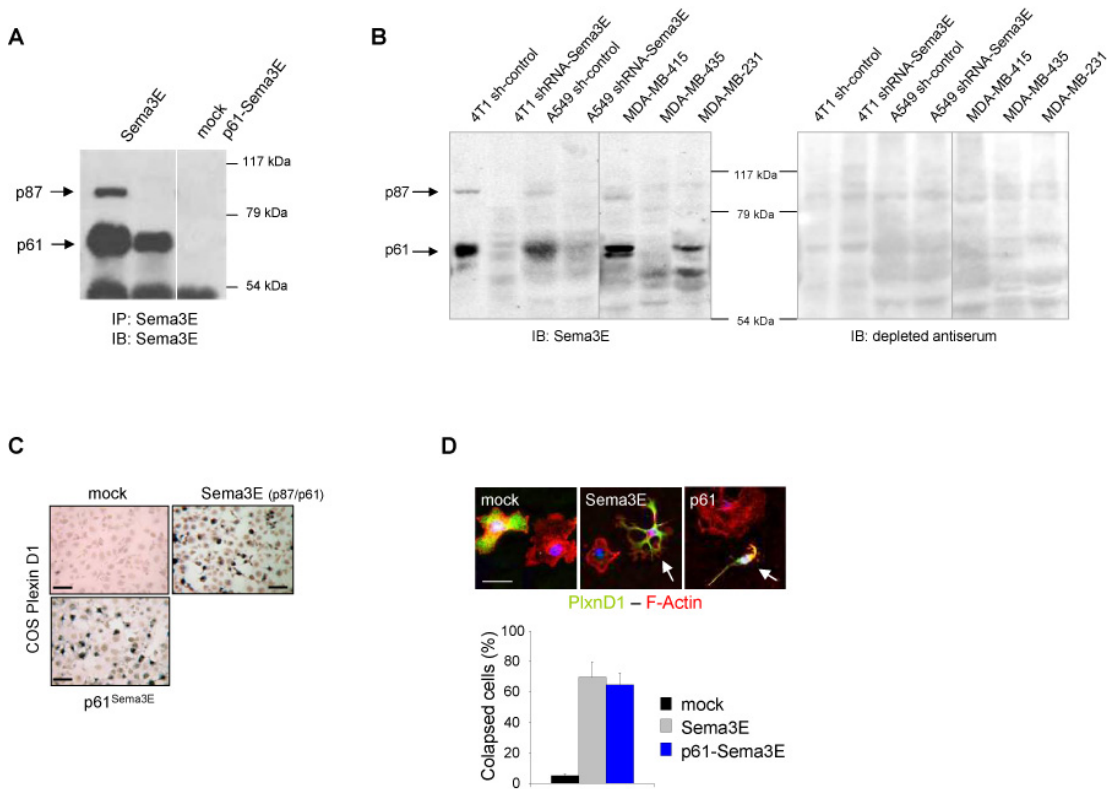
Figure S2



A-B. *Sema3E* expression was silenced in A549 tumor cells by expressing two distinct shRNA sequences (I and II; see Suppl. Table 1), and the cells were used to establish subcutaneous tumor xenografts. 60 days after injection, we scored tumor weight (A) and the formation of spontaneous metastasis in the lungs (B). The two independent shRNA sequences targeting *Sema3E* transcript have similar effects in cancer cells; ** $p < 0.005$. Notably, shRNA (I) is that used in the experiments shown in Fig. 1D-L.

C. Sema3E expression was knocked down in HCT-116 colon carcinoma cells by RNAi. Sema3E-deficient cells did not show any change in viability, growth rate in culture or tumorigenicity in mice (data not show); however, their ability to form experimental metastatic colonies in the lungs upon injection in the circulation was dramatically impaired; ** $p < 0.001$.

Figure S3



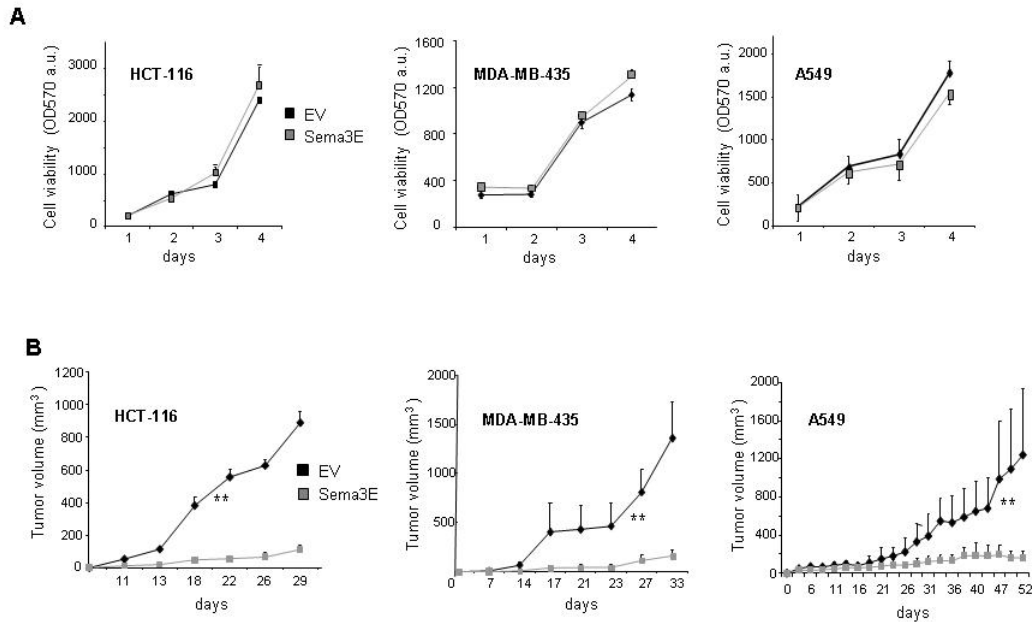
A. MDA-MB-435 tumor cells were transduced to express full-length Sema3E or the truncated form p61. The expression and proteolytic processing of the semaphorin was verified by anti-Sema3E immunoblotting.

B. Anti-Sema3E immunoblotting analysis (left picture) of conditioned media harvested by several tumor cell lines (grown in absence of fetal serum), either wild type or transduced with gene-targeted shRNA to knock-down Sema3E expression. Comparable amounts of total proteins were loaded in the different lanes. Arrows on the left indicate bona fide identification of the full-length precursor p87-Sema3E and the proteolytic fragment p61. The same filters were stripped and incubated with antigen-depleted anti-Sema3E antibodies to confirm band specificity (shown on the right).

C. COS cells transfected with PlexinD1 were probed with the indicated AP-bound molecules (approx. 7nM each) to reveal receptor binding (details in Methods section). Both the product of processable wild-type Sema3E (yielding a mix of p87/p61 isoforms), and the recombinant p61-Sema3E fragment are competent to bind PlexinD1 and induce cell collapse. Scale bar: 60 μ m. The collapsing response was further revealed by immunofluorescence, as described below.

D. COS cells transfected with PlexinD1 (as above) were incubated with the indicated molecules (approx. 7nM each) for approx. 1 hour. Cellular collapse was revealed as previously described (Barberis et al., 2004). Briefly, the cells were fixed and analyzed by immunofluorescence to identify (myc-tagged) PlexinD1-expressing cells (in red), and with Falloidin-FITC to reveal F-Actin. Collapsed cells (indicated by arrows in representative fields) were identified for having a diameter equal or less than 30 μ m. Both full length Sema3E and p61 truncated fragment are equally competent to trigger cell collapse. Scale bar: 30 μ m.

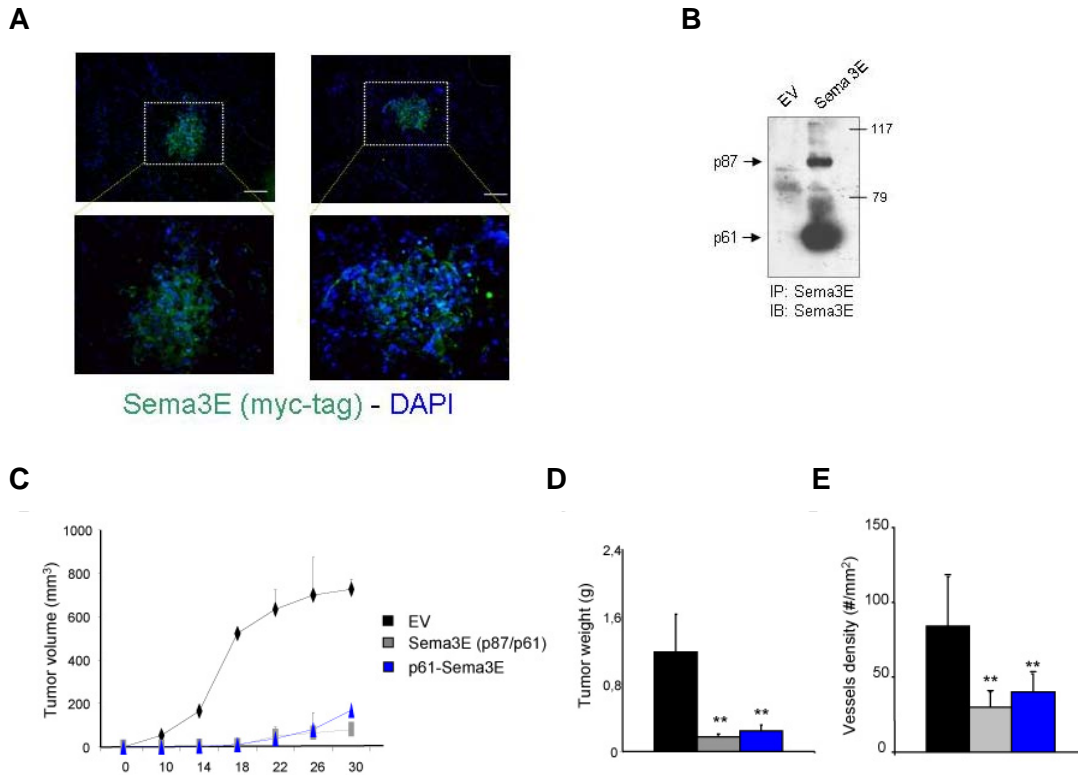
Figure S4



A. HCT-116 colon carcinoma, MDA-MB-435 melanoma and A549 lung carcinoma cells (as indicated in the figure), transduced with lentiviral vectors to express Sema3E or a non-coding empty vector (EV), were grown in culture for four days in 0.1% FBS. Cell viability was evaluated daily, by staining with MTT and quantifying absorbance at 570nm. Data shown represent the average of triplicates \pm SD.

B. The same cells as above were transplanted subcutaneously in nude mice. The graph displays the growth of tumor volume, measured externally during the experiment. Data shown represent the average \pm SD of six mice per each experimental condition; ** $p < 0.05$.

Figure S5



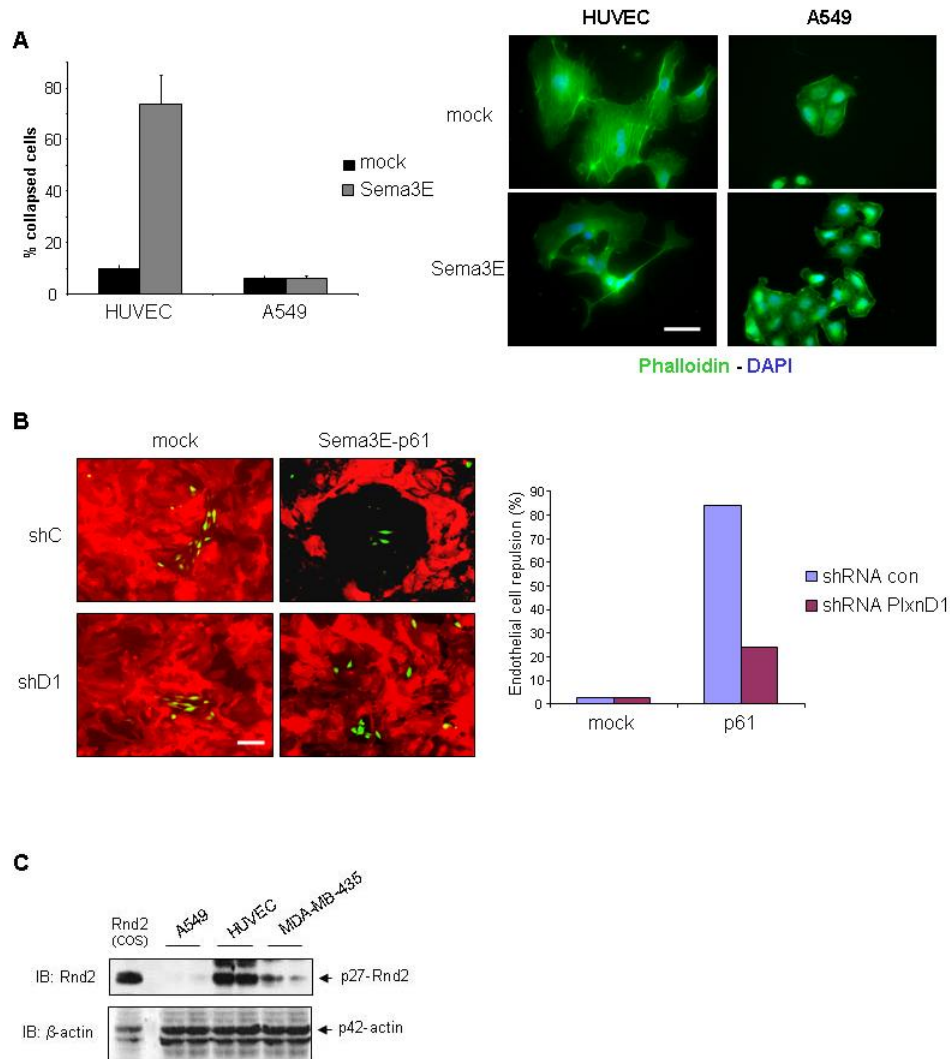
A. Immunofluorescence analysis revealing the expression of Sema3E (myc-tagged) in secondary metastatic foci in the lungs of mice bearing Sema3E-overexpressing MDA-MB-435 primary tumors. Two representative images are shown: low magnification on top (scale bar: 100 μ m) and higher magnification at the bottom.

B. Anti-Sema3E immunoblotting of lysates derived from MDA-MB-435 tumor xenografts overexpressing Sema3E full-length and the respective controls (described in Fig. 2B-G). The majority of Sema3E has been converted by PPC in vivo into p61 fragment.

C-D. MDA-MB-435 cells transduced with wild-type Sema3E, p61, or EV-control (protein expression shown in Fig. S3A) were injected subcutaneously into nude mice. Graphs display tumor volume (A) and tumor weight at 4 weeks from injection (B). Data are given as average \pm SD of five mice for each experimental group; ** $p < 0.002$.

E. Tissue sections of tumor xenografts above were stained with anti-CD31 to reveal endothelial cells. Values in the graph indicate the vessel density (average \pm SD); ** $p < 0.005$.

Figure S6



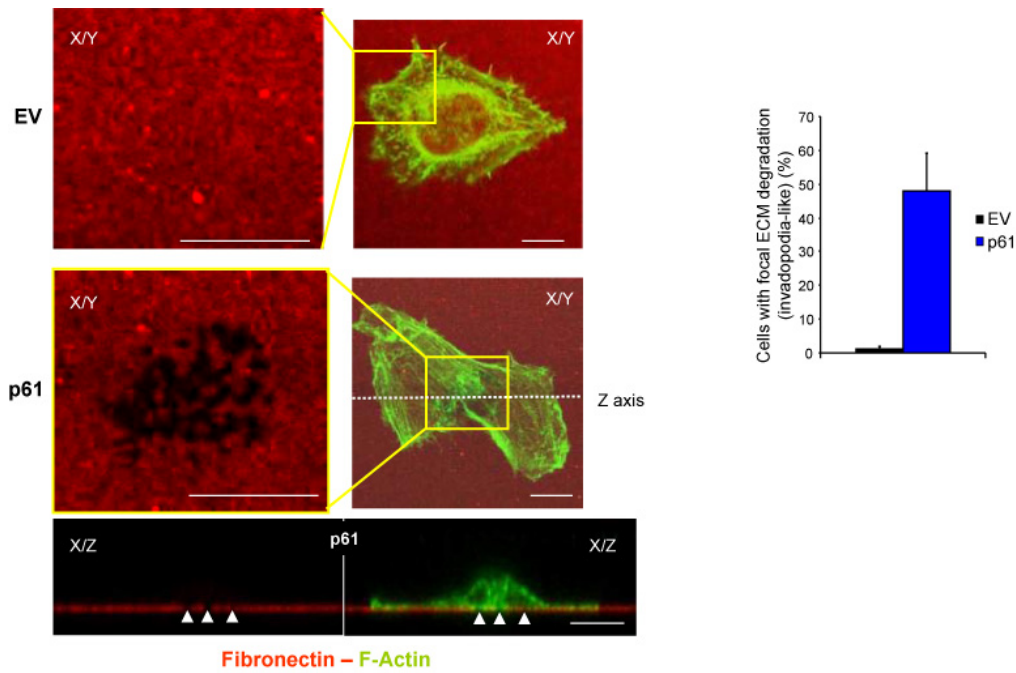
A. HUVEC or A549 cancer cells in culture were incubated for 4 hours in the presence of Sema3E-containing or mock conditioned medium. Cells were then fixed and stained with DAPI and Falloidin-FITC to reveal the nuclei and F-actin, respectively. Micrographs show representative fields. Sema3E induced the retraction of cellular processes and a typical collapsed phenotype (Barberis et al., 2004) in endothelial cells, while A549 were unaffected (or displayed increased lamellipodia). Scale bar: 30 μ m.

B. Immunofluorescence analysis of the coculture of MDA-MB-435 tumor cells transduced to express Sema3E EV-control on a monolayer of Human Umbilical Vein

Endothelial cells (HUVEC) grown on glass coverslip (see Suppl. Methods for details). Before seeding, tumor cells had been labeled with Vybrant green cell tracker, while HUVEC were revealed by immunostaining with a-human CD31 (red) at the end of the experiment. Micrographs show representative fields. The expression of Sema3E in tumor cells induced the repulsion of HUVEC disrupting their monolayer, dependent on the expression of PlexinD1 in endothelial cells. Scale bar: 100 μ m.

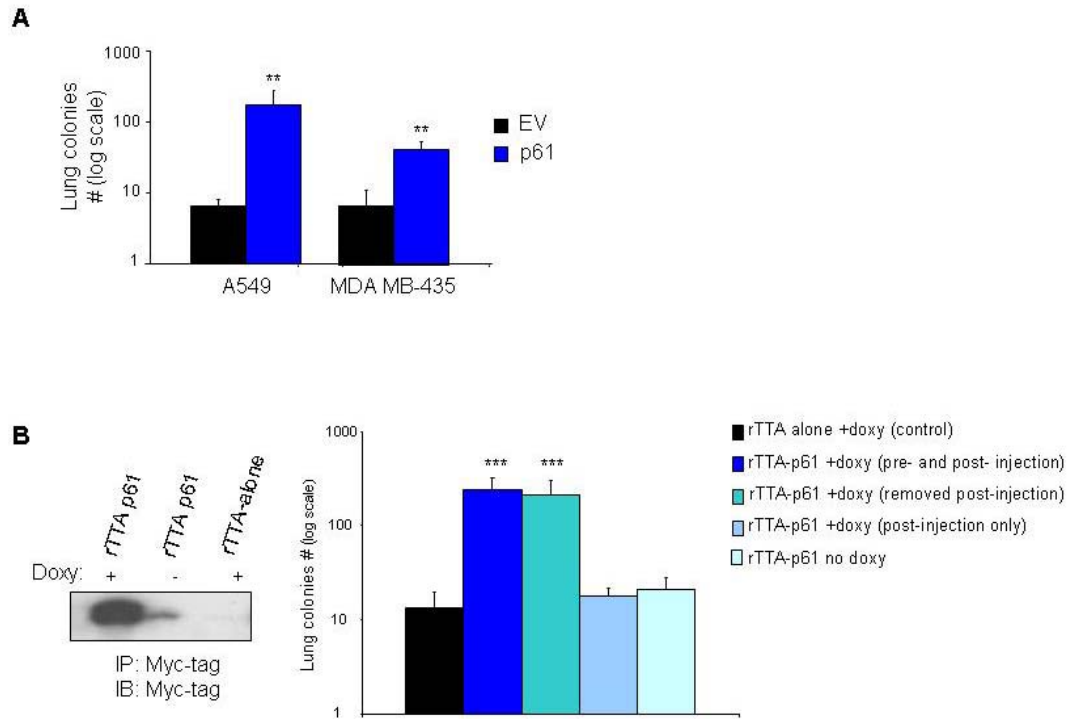
C. Rnd2 expression was analyzed by immunoblotting in protein lysates derived from endothelial cells HUVEC and tumor cells A549 and MDA-MB-435. Lysates of COS cells transfected with Rnd2 cDNA provided a positive control for band specificity and β -actin expression analysis (at the bottom) provided an internal loading control. Endothelial cells contain a much larger amount of Rnd2 compared to the analyzed tumor cells. Analogous results were obtained by real time Q-PCR analysis (not shown).

Figure S7



MDA-MB-435 tumor cells expressing p61-Sema3E (or controls) were incubated on glass coverslips coated with fluorescent ECM (labeled in red; see Methods) for 16 hours. After cell fixation, F-actin was stained with phalloidin-FITC (merged images on the right). Localized matrix degradation was identified by confocal microscopy as dark areas within the red ECM layer (see close-up images on the left). The fraction of cells presenting this phenotype was scored in a number of fields, and the results are shown in the graph at the bottom-left corner. Bottom images show a representative “x-z” projection of the same field of p61-cells shown in the middle; they contained invadopodia-like structures (indicated by arrowheads), characterized by actin-rich processes (labeled in green) colocalizing with focal spots of extracellular matrix degradation. Scale bars: 10 μ m.

Figure S8

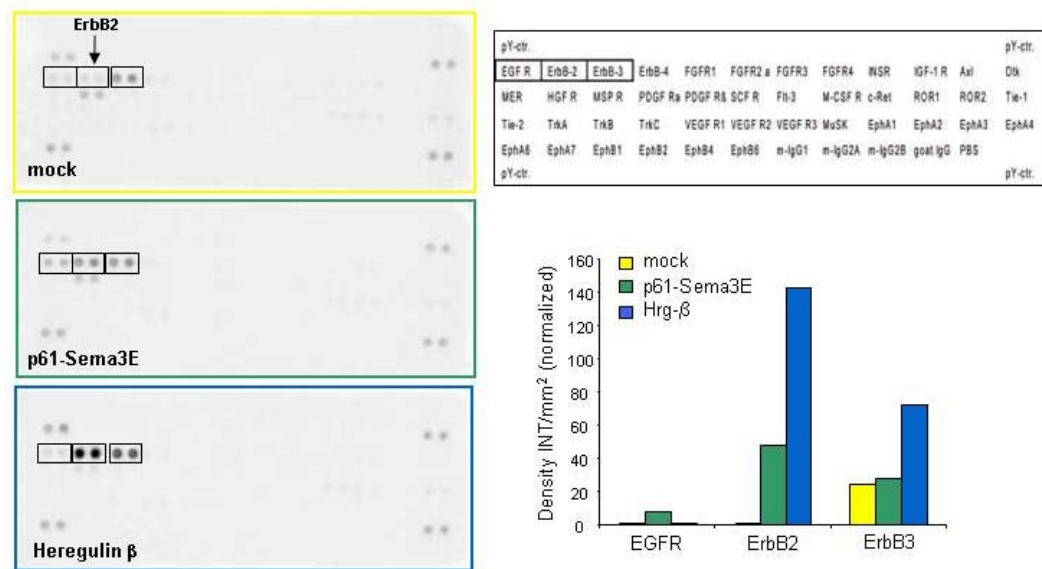


A. Control-EV or Sema3E-overexpressing cells (either A4549 or MDA-MB-435, as indicated) were injected intravenously in nude mice, and lung metastatic colonies were counted 30 days after injection (see Methods); the graph shows average values \pm SD of eight mice for each experimental condition; Y-axis is in logarithmic scale; ** $p < 0.005$.

B. A tetracyclin-regulated system was used to achieve rapid induction of Sema3E expression in tumor cells (see validation by western blot analysis, on the left). We then performed an experimental metastasis assay by injecting engineered A549 cells in the tail vein of nude mice. Five experimental groups were analyzed: mice in group I received cells transduced with rTTA control vector, to reveal their basal metastatic potential. Mice in group II were injected with cells carrying Sema3E-p61 inducible construct that have been pre-treated with doxycycline to induce semaphorin expression before injection, and were kept under treatment with the drug thereafter during the entire experiment. Group III comprised mice injected with the same cells as above, but for drug-treatment was terminated four days after tumor cells injection. Mice in group IV and V received tumor cells not pre-treated with doxycycline; thus these cells did not express Sema3E at the

time of injection. However, in group IV, *Sema3E* expression was induced four days after injection, when spontaneous tumor cell extravasation in lungs has already occurred, whereas mice in group V were never treated with doxycycline. After one month from injection we scored the number of lung colonies, and observed that exclusively the mice in group II and III, which received cancer cells expressing *Sema3E* at time of injection, had developed a significantly higher number of metastatic foci, compared to control groups. Instead, mice in group IV, for which semaphorin expression in tumor cells was induced immediately after extravasation, displayed a negligible increase in lung colonies with respect to controls (graph on the right); Y-axis is in logarithmic scale; *** $p < 0.001$. Thus, *Sema3E*-p61 specifically acts by promoting tumor cell extravasation and it is not effectively sustaining cancer cell growth or survival in the lung tissue at later stages.

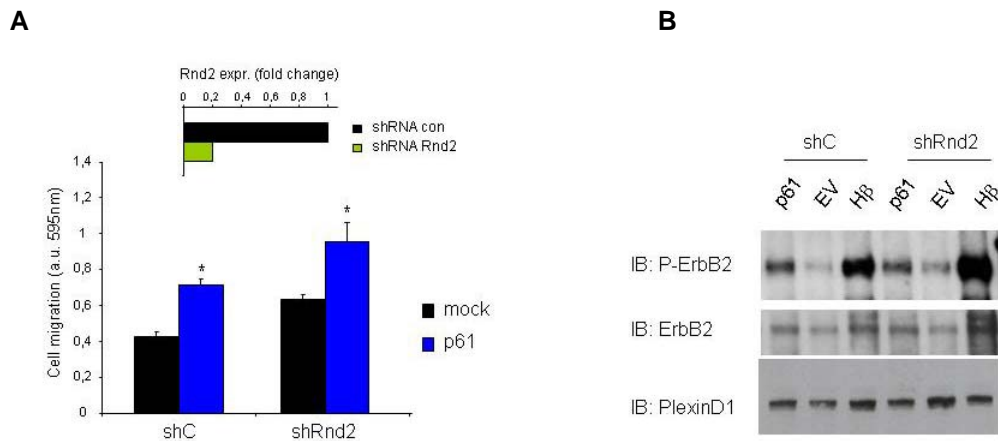
Figure S9



The tyrosine phosphorylation of 42 tyrosine kinase receptors was simultaneously assessed in protein lysates of A549 tumor cells treated for 15 minutes with 7nM p61-Sema3E or 0.2nM Hrg-β, using a Phospho-RTK Array (R&D) according to

manufacturer's protocol. Chemiluminescence-labeled arrays were scanned using FUJI FILM LAS-4000 Image Capturing Unit, and pixel density in each spot of the array was analyzed using ImageJ analysis software (graph on the right). The signal of individual spots detected in each filter was normalized to the average of positive control spots in the array (vs. background).

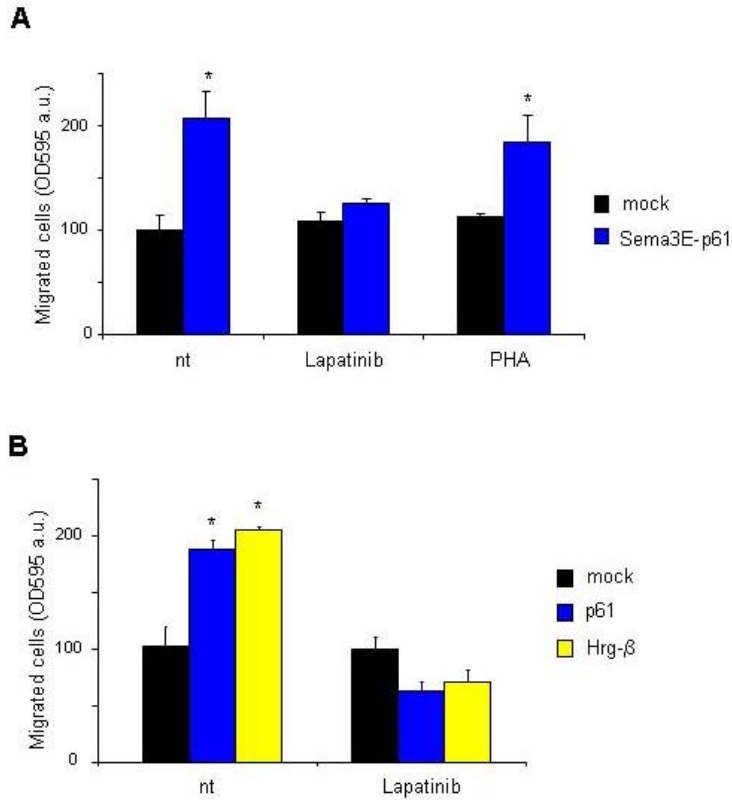
Figure S10



A. Sema3E-p61-induced migration of A549 carcinoma cells stably expressing shRNA to knock down Rnd2 levels, and respective controls (Q-PCR analysis shown on top). Migrated cells were detected as in other experiments (see Methods) and values were normalized to control.

B. p61-induced tyrosine phosphorylation of ErbB2 in the same cells as above. Experimental conditions are the same as in Fig. 8A; Heregulin-β1 (Hβ) provided a positive control for ErbB2 activation.

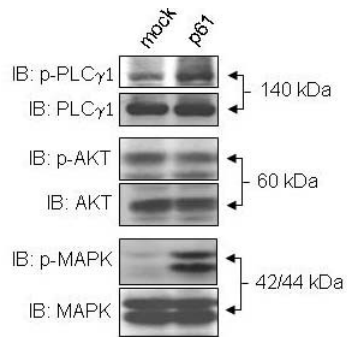
Figure S11



A. MDA-MB-435 cells were pretreated with 400nM Lapatinib (ErbB2 inhibitor) or 250nM PHA-665752 (Met inhibitor) for 2 hours. Thereafter, these cells were added in the upper chamber of Transwell inserts, in presence of the same tyrosine kinases inhibitors, and allowed to migrate in response to 7nM p61-Sema3E. Migrated cells were stained with crystal violet; the dye was eluted and quantified by absorbance at 595nm (see Methods for details). Data are given as average \pm SD of two independent experiments; * p <0.05.

B. HeLa cells were pretreated with Lapatinib (400nM) for 2 hours; subsequently, their migration was assayed in Transwell inserts, in presence of 7nM p61-Sema3E or 1nM Hrg- β . Migrated cells were quantified as above. Data are given as average \pm SD of two independent experiments; * p <0.05.

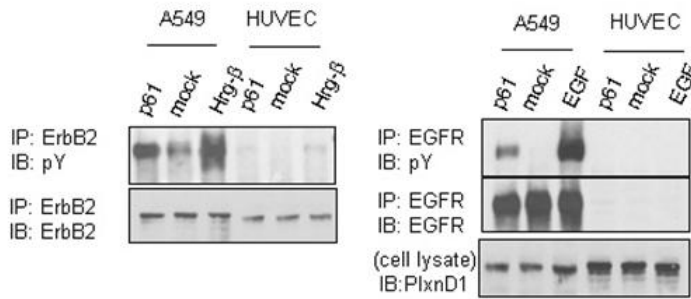
Figure S12



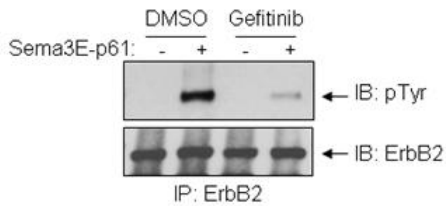
A549 carcinoma cells were treated with 7nM purified Sema3E-p61 for 20 minutes. Total protein lysates were then analyzed by Western blotting with phospho-specific antibodies to detect activated forms of PLC γ 1 (Y783), MAPK and AKT, as well as with the respective non-phospho-specific antibodies to provide loading controls. p61 selectively induced activation of MAPK and PLC γ 1 but not AKT.

Figure S13

A



B



A. A549 carcinoma cells and HUVEC endothelial cells were treated with 7nM p61-Sema3E, 0.2 nM Heregulin- β 1, 1nM EGF, or mock for 15 min (as for experiments shown in Fig. 7A-C). Cell lysates were then immunopurified with anti-EGFR or anti-ErbB2 antibodies (as indicated) and subjected to immunoblotting to reveal tyrosine kinase expression and phosphorylation levels. Equal protein levels in the lysates were confirmed using anti-PlexinD1 antibody (bottom row on the right). ErbB2 and EGFR, which are co-expressed in cancer cells but not in endothelial cells, become tyrosine phosphorylated in response to p61-Sema3E.

B. Serum starved HeLa cells were pre-treated for 3 hours with the specific EGFR inhibitor Gefitinib (500nM) or with vehicle (DMSO), and stimulated for 15 minutes with 7nM p61 (similarly to that shown in Fig. 6C, main manuscript). ErbB2 was immunopurified from cell lysates and the effects of Gefitinib on tyrosine phosphorylation were visualized using specific antibodies.

SUPPLEMENTAL METHODS

Patients and tissues

Tissue samples for RNA extraction and subsequent quantitative RT-PCR were obtained from patients undergoing resection of primary colorectal adenocarcinoma or liver metastases from colorectal carcinoma at the University of Heidelberg, Department of Visceral Surgery, between 2006 and 2008. All tissue samples were snap frozen immediately after resection and stored at -80°C until further analysis was performed. The following specimens were included in this analysis: 43 primary tumors that had not formed distant metastases (*M0* stage according to TNM classification for colorectal cancer), 17 primary colorectal tumors that had formed distant metastases at the time of resection (*M1* stage), and 51 liver metastases. Unless otherwise indicated, the Wilcoxon test was regularly applied for expression analyses in clinical samples.

Cell lines

Tumor cell lines were from ATCC. Human umbilical vascular endothelial cells (HUVECs) were from Clonetics. Tumor cell lines were grown in standard medium supplemented with with L-glutamine and 10% FBS (Sigma), whereas HUVECs were grown in Endothelial Cell Basal Media from Lonza.

RNAi mediated gene silencing and gene expression analysis by qPCR

Lentiviral vectors were used to express gene-targeted shRNA sequences identified by computer-assisted analysis (or an unrelated sequence as negative control) under the transcriptional control of the H1 promoter derived from pSUPER plasmid (Brummelkamp et al., Science 2002)(see below). Gene silencing was validated by Real Time qPCR (see below). The knock-down of Met expression was similarly achieved, as described (Corso et al., 2008). Rnd2 expression was knocked down in HUVEC by transfection with siRNA duplexes ON-Target Plus SMART pool (L-009727-00-0010; Dharmacon-Thermo Scientific) or siCONTROL nontargeting siRNA pool (D-001206-

13), using Lipofectamine 2000 (Invitrogen), according to manufacturer's protocols and previous reports (Valdembri et al., 2009). Briefly, the cells were transfected twice (at 0 and 24 h) with 200 pmol of siRNA duplexes; after 24 hours since the second oligofection, cells were used in functional assays and assayed in parallel by Real Time Q-PCR.

Targeted gene	Sequence targeted by shRNA
PLXND1 (I) (<i>human</i>)	5'-ACGGCAAGCTGGAGTACTA-3'
PLXND1 (II) (<i>human</i>)	5'-TTCTCAAGATCAACCTGAA-3'
SEMA3E (I) (<i>human</i>)	5'-GGTTACGCCTGTCACATAA-3'
SEMA3E (II) (<i>mouse/human</i>)	5'-TGCTGAAAGTAATCACAAT-3'
HER2-ErbB2 (<i>human</i>)	5'-TCACAGGGGCTCCCCAGG-3'

TaqMan Gene Specific Probes

Gene symbol	Assay ID	Ref. Seq.
h-SEMA3E	Hs00180842_m1	NM_012431.1
h-PLXND1	Hs00391129_m1	NM_015103.1
h-ACTB	Hs99999903_m1	NM_0011012

SYBR Gene Specific Primers

Gene symbol	Ref. Seq.	Fw. Sequence (5'-3')	Rev. Sequence (5'-3')
h-SEMA3E	NM_012431	CGGGGCACATTATCACCT	CCAGCAGCATTGTATGGAGA
h-RND2	NM_005440.4	CTCAAGAGTTCTGCCCAAT	AGTGCCCTGCTCATGTGTAA
h-GAPDH	NM_002046	GAAGGTGAAGGTCGGAGTC	GAAGATGGTGATGGGATTC
m-sema3E	NM_011348	CTGTGCCTTCATCAGAGTCG	GGAGGAGTTGGGGTCAAAA
m-actinb	NM_007393	GCTCTTTTCCAGCCTTCCTT	TCTCCTTCTGCATCCTGTCA

Immunoprecipitation, SDS-PAGE and Western Immunoblotting

Cellular proteins were analyzed by standard methods, briefly described in Supplemental materials. Cellular proteins were solubilized in EB-extraction buffer (20 mM Tris-HCl pH 7.4, 150 mM NaCl, 10% Glycerol, 1% TritonX-100) or RIPA buffer (50 mM Tris-HCl pH 7.4, 150 mM NaCl, 0.1% Sodium Dodecyl Sulfate, 0.25% Na-Deoxycholate, 1% TritonX-100), additionated with 1 mM Na₃VO₄, 100 mM NaF, 1 mM PMSF, 10 µg/ml leupeptin, 10 µg/ml aprotinin, 1 µg/ml pepstatin. When appropriate, the total protein concentration in cell lysates was determined by BCA assay (Pierce). Protein

immunoprecipitation was performed by incubation with ProteinA-Sepharose beads and appropriate antibodies. Immunopurified proteins or equal amounts of total cellular lysates were separated by SDS-PAGE, transferred to nitrocellulose membranes, and blocked in phosphate-buffered saline, 0.1% Tween, 10 % BSA. The membrane was then incubated with primary antibodies, followed by the appropriate peroxidase-conjugated secondary antibody (Bio-Rad). Final detection was done by enhanced chemiluminescence (ECL, Amersham Biosciences). Phospho-specific antibodies to detect activated MAPK, AKT, PLC γ 1 (Y783), as well as respective non-phospho-specific antibodies were from Cell Signaling.

Sema3E-receptor binding and collapse assays

Sema3E expression constructs were subcloned in frame with Secreted Placental Alkaline Phosphatase (SeAP) and transfected in COS cells to obtain molecular probes to be used in PlexinD1 binding and collapse assays. In situ binding assays were performed as described previously (Tamagnone et al., Cell 1999). Briefly, Plexin D1-expressing COS cells were incubated for 1 h with recombinant secreted Sema3E or p61 fragment fused to AP. After five washes, cells were fixed, heated for 10 min at 65°C to inactivate endogenous phosphatases, and incubated with NBT-BCIP (nitro blue tetrazolium-5-bromo-4-chloro-3-indolyl-phosphate) AP substrate (Promega). Cell collapse assays were performed as described previously (Barberis et al., 2004). Briefly, Plexin D1-expressing COS cells were incubated for 1 h with recombinant secreted Sema3E or p61 fragment, then fixed with 4% PAF, permeabilized with 0.1% TritonX100 and immunostained to reveal PlexinD1.

Immunohistochemistry analysis on human samples

Formalin-fixed and paraffin-embedded naevi and melanoma samples, prepared for routine histopathological analysis, were derived from therapeutical surgical excisions at the Institute for Cancer Research and Treatment (IRCC) of Candiolo, Torino. A series of 68 samples analyzed for this work included: intradermal naevi (n=12), junctional naevi (n=8), dysplastic nevi (low grade n=5 and severe grade n=8), melanomas in situ (n=5), primary cutaneous melanomas (Clark level II, n=5; Clark III, n=6; Clark IV, n=10). Tissue

sections (4 μm thick) were processed in a PT link station (DAKO Denmark) and subjected to EnVision Flex Target Retrieval Solution low pH. The specimens were immuno-stained with anti-Sema3E antibody (Christensen et al., 2005; dilution 1:800) and revealed by the EnVision Flex detection system (DAKO), using diaminobenzidine as chromogen. Tissue sections were counterstained with hematoxylin. Sema3E expression in each sample was scored semi-quantitatively, based on the fraction of cells displaying cytoplasmatic or membranous staining, out of minimum 500 cells counted in six non-contiguous microscopic fields per sample.

Co-culture assays with HUVEC and tumor cells

HUVEC repulsion by semaphorin-releasing tumor cells was analyzed as described previously (Bielenberg et al., 2004) with the following modifications. HUVECs were grown to confluence on gelatine-coated coverslip in 24-well cell culture dishes. The endothelial cell monolayer was incubated with 200nM DiI (Molecular Probes) for 30' and then washed twice with PBS. 6×10^3 MDA MB-435 tumor cells carrying sema3E or Sema3A (positive control) or EV were fluorescently labeled with Vybrant® (Molecular Probes) and incubated onto HUVEC monolayer for 48 hours. Cells were then fixed with PAF and analyzed with LEICA DMI3000 fluorescent microscope at low magnification.

Inducible expression of Sema3E in tumor cells

Regulated expression of Sema3E-p61 was achieved by transducing tumor cells with a lentiviral expression construct under control of a rTTA- and doxycycline-regulated promoter (generously provided by Elisa Vigna, IRCC, Torino; Vigna et al. 2002). Semaphorin expression was induced by adding doxycycline in cell culture medium (0.1-1mg/ml) and in the drinking water of mice (1mg/ml).

ECM degradation assay and invadopodia detection

Fluorescent matrix-coated coverslips were prepared as described previously (Lorenz M. et al Curr. Biol. 2004). Briefly, thin layers of 2.5% gelatine and 2.5% sucrose in PBS were placed on glass coverslips, air-dried for 1h and crosslinked with 0.5% glutaraldehyde for 10 min at 0° C. After extensive wash with PBS, coverslips were

overlayed with 50 mg/ml Rhodamine-Fibronectin (Cytoskeleton Inc. Denver CO.USA) and incubated for 1h at 37°C. Finally, after incubation with ethanol 70% for 10', coverslips were quenched with complete growth medium (DMEM 10%FBS) for 30' before cell plating. Approx. 5×10^3 MDA-MB-435 cells were cultured on FN-gelatin-coated glass coverslips for 16 h. At the end of the experiment, the cells were fixed and F-actin was stained with fluorescein-labeled phalloidin (Sigma). Slides were analyzed with a confocal laser-scanning microscope LEICA TCS SP2 and z axes reconstruction were optimized using Leica confocal software.

Phosphoproteomic macroarray

The phosphorylation of multiple receptor tyrosine kinases was detected using the Proteome Profiler Array Kit ARY001 (R&D Systems, Minneapolis, MN, USA), according to manufacturer's protocols.

SUPPLEMENTAL REFERENCES

- Barberis, D., Artigiani, S., Casazza, A., Corso, S., Giordano, S., Love, C.A., Jones, E.Y., Comoglio, P.M., Tamagnone, L. (2004). Plexin signaling hampers integrin-based adhesion, leading to Rho-kinase independent cell rounding, and inhibiting lamellipodia extension and cell motility. *FASEB J.* 18, 592-594.
- Bielenberg, D.R., Hida, Y., Shimizu, A., Kaipainen, A., Kreuter, M., Kim, C.C., Klagsbrun, M. (2004). Semaphorin 3F, a chemorepellent for endothelial cells, induces a poorly vascularized, encapsulated, nonmetastatic tumor phenotype. *J. Clin. Invest.* 114, 1260-1271.
- Brummelkamp, T.R., Bernards, R., Agami, R. (2002). A system for stable expression of short interfering RNAs in mammalian cells. *Science* 296, 550-3.
- Corso, S., Migliore, C., Ghiso, E., De Rosa, G., Comoglio, P.M., Giordano, S. (2008). Silencing the MET oncogene leads to regression of experimental tumors and metastases. *Oncogene* 27, 684-693.
- Lorenz, M., Yamaguchi, H., Wang, Y., Singer, R.H., Condeelis, J. (2004). Imaging sites of N-wasp activity in lamellipodia and invadopodia of carcinoma cells. *Curr. Biol.* 14, 697-703.
- Tamagnone L, Artigiani S, Chen H, He Z, Ming GI, Song H, Chedotal A, Winberg ML, Goodman CS, Poo M, et al. (1999). Plexins are a large family of receptors for transmembrane, secreted, and GPI-anchored semaphorins in vertebrates. *Cell* 99, 71-80.
- Valdembri, D., Caswell, P.T., Anderson, K.I., Schwarz, J.P., König, I., Astanina, E., Caccavari, F., Norman, J.C., Humphries, M.J., Bussolino, F., Serini, G. (2009). Neuropilin-1/GIPC1 signaling regulates alpha5beta1 integrin traffic and function in endothelial cells. *PLoS Biol.* 7, 1.
- Vigna, E., Cavalieri, S., Ailles, L., Geuna, M., Loew, R., Bujard, H., Naldini, L. (2002). Robust and efficient regulation of transgene expression in vivo by improved tetracycline-dependent lentiviral vectors. *Mol. Ther.* 5, 252-261.